Implementation of On-the-Fly Doppler Broadening in MCNP

William R. Martin and Scott Wilderman
Department of Nuclear Engineering and Radiological Sciences
University of Michigan
wrm@umich.edu; sjwnc@umich.edu

Forrest B. Brown
Los Alamos National Laboratory
fbrown@lanl.gov

Gokhan Yesilyurt
Argonne National Laboratory
gyesilyurt@anl.gov

ABSTRACT

A new method to obtain Doppler broadened cross sections has been implemented into MCNP, removing the need to generate cross sections for isotopes at problem temperatures. When a neutron of energy E enters a material region that is at some temperature T, the cross sections for that material at temperature T are immediately obtained "on-the-fly" (OTF) by interpolation using a high order functional expansion for the temperature dependence of the Doppler-broadened cross section for that isotope at the neutron energy E. The OTF cross sections agree with the NJOY-based cross sections for all neutron energies and all temperatures in the range specified by the user, e.g., 250K - 3200K. The OTF methodology has been successfully implemented into the MCNP Monte Carlo code and has been tested on several test problems by comparing MCNP with conventional ACE cross sections versus MCNP with OTF cross sections. The test problems include the Doppler defect reactivity benchmark suite and two full-core VHTR configurations, including one with multiphysics coupling using RELAP5-3D/ATHENA for the thermal-hydraulic analysis. The comparison has been excellent, verifying that the OTF libraries can be used in place of the conventional ACE libraries generated at problem temperatures. In addition, it has been found that the OTF methodology greatly reduces the complexity of the input for MCNP, resulting in an order of magnitude decrease in the number of input lines for full-core configurations. Finally, for full-core problems with multiphysics feedback, the memory required to store the cross section data is considerably reduced with OTF cross sections and the additional computational effort with OTF is modest, on the order of 10-15%.

Key Words: Doppler broadening, Monte Carlo, on-the-fly, multiphysics

1. INTRODUCTION

Doppler broadening of nuclear cross sections is a key nuclear phenomenon that occurs during nuclear reactor operation and has important implications for reactor safety. Resonance cross sections change significantly due to the relative motion between the incoming neutron and the target nucleus and must be accounted for in the analysis of reactors at operating temperature. If a continuous energy Monte Carlo code such as MCNP [1] is used for the neutronics portion of a multi-physics simulation with thermal-hydraulic feedback, cross section libraries must be generated for all isotopes over the range of temperatures expected in the reactor. In a light water reactor (LWR), this process can result in tens of thousands of material temperatures for which

broadened cross sections need to be generated using NJOY [2]. Since a cross section file for a typical isotope at a specified temperature may be 10 MB in size, this can result in a huge increase in fast memory to store the cross section files. Moreover, the need to assign different material IDs to cross section files for the same isotope at different temperatures greatly complicates (and expands) the input files for problems with temperature feedback.

Previous research by Yesilyurt et al. [3-5] demonstrated the feasibility of replacing the cross section files generated at specific temperatures with functional expansions that represent the detailed energy and temperature dependence of the cross sections. This allowed "on-the-fly" (OTF) determination of Doppler-broadened cross sections at the exact temperatures encountered by the neutron during its random walk through the problem geometry.

The goal of a project supported by DOE was to take the OTF capability beyond the scientific feasibility stage and extend it to a production capability by incorporating it into the MCNP Monte Carlo code, providing reactor analysts the capability to analyze coupled neutronic/TH calculations without the need to generate cross section libraries at all temperatures that are anticipated during the simulation. This paper is drawn from the final report [6] for this project.

2. OTF METHODOLOGY

2.1. Overall Description

The basic idea is to expand the temperature dependence of a particular cross section at a given neutron energy in a functional expansion in temperature for every nuclide and every cross section type that is subject to Doppler broadening. The expansion coefficients are a function of isotope, cross section type, and energy grid point E_g. For example, the capture cross section for a given isotope at a given energy grid point E_g might have the following temperature expansion:

$$\sigma_\gamma\left(T,E_g\right) \cong \sum_{i=1}^{N} \frac{a_{g,i}}{T^{i/2}} + \sum_{i=1}^{N} b_{g,i} T^{i/2} + c_g \qquad (1)$$

The expansion coefficients $a_{g,i}$, $b_{g,i}$, and c_g are determined by a temperature-dependent regression model based on the exact Doppler broadened cross sections [6] at that energy grid point. These coefficients allow the determination of cross sections for all neutron energies and all temperatures over an arbitrary temperature range determined by the analyst who generates the OTF library. We have found that N=8 (corresponding to a 17 term expansion) yields agreement with NJOY-determined cross sections to within 0.1% for all cross section types over the entire energy and temperature range specified for the OTF library. The following sections summarize the OTF methodology that was implemented into MCNP. Detailed descriptions of the OTF implementation and results can be obtained from [6].

2.2. Creating a Union Energy Mesh for an Isotope

The first step is to construct a union energy grid over a predefined temperature range of interest for each of the isotopes. Here, "union" refers to a common energy grid structure for a single isotope that can be used for all of the broadened cross sections for that isotope while maintaining

satisfactory agreement with the exact cross section values. For example, U-238 will have all of its cross sections, including temperature-dependent cross sections over the specified temperature range (e.g., 250K - 3200K), tabulated on the same grid. The determination of the union energy grid is based on satisfying the NJOY fractional tolerance (FT) for all of these cross sections and temperatures. The FT is defined as the relative difference in cross sections between the values of exact and linearly interpolated cross sections at mid-points between successive energy grid points. Thus the energy grid spacing $\Delta E = E_2 - E_1$ satisfies the FT criterion if

$$\frac{\left|\sigma^x_{exact} - \sigma^x_{lin}\right|}{\sigma^x_{exact}} < FT \qquad (2)$$

The user specifies a union temperature grid with specified spacing ΔT_{union} which is used for all cross sections and all isotopes in the OTF library. The union temperature grid is only used to generate the union energy grid and is not used after that.

Figure 1 illustrates why the union energy grid is important. When the temperature increases, the number of energy grid points required to satisfy a given FT decreases near the peak of a resonance as it smooths out, resulting in a coarser energy grid structure. However, when the temperature increases, more energy grid points are required for the middle and wings of a resonance to satisfy the same FT, yielding a finer energy grid structure. By construction, energy grid points are only added to the union energy grid, and never taken away, so the overall effect is a modest increase in energy grid points with temperature as a result of the increased energy resolution needed for the middle and wings of the resonances as the temperature increases.

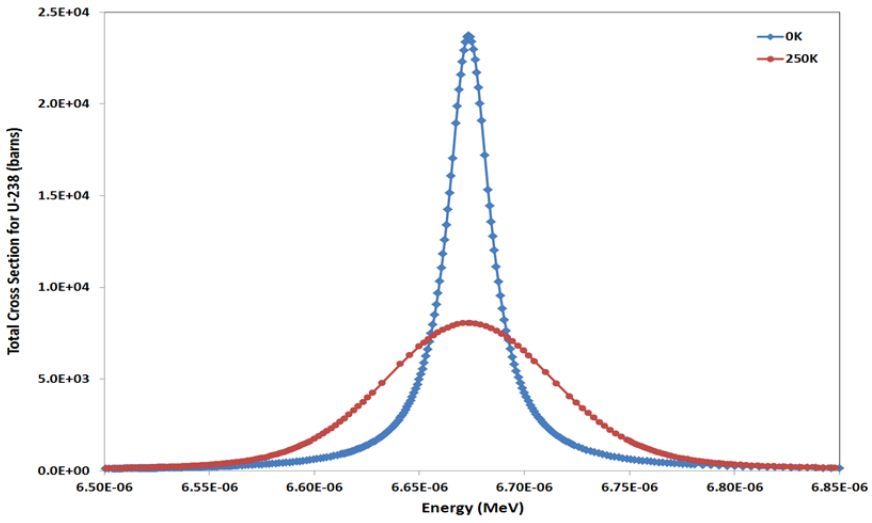

Figure 1. Evolution of U-238 Cross Section Energy Grid with Temperature.

The initial union energy grid corresponds to the base set of cross sections that have been generated by NJOY at a specified temperature and satisfies Eq. (2) by construction. The construction of the union energy grid for a specific isotope then consists of a loop over the

energy grid, with an inner loop over the union temperature points and cross section types for that isotope, halving the current energy grid spacing until Eq. (2) is satisfied for every temperature and cross section type. The end result is an energy grid that is unique for each isotope and satisfies Eq. (2) for all temperatures and cross section types.

For example, the starting energy grid for U-238 had 134,437 energy points and an additional 10,866 energy grid points had to be added to satisfy Eq. (2) for capture, elastic scattering, fission, and total cross sections, in that order.

2.3. Determining Doppler-Broadened Cross sections on the Union Energy Grid

The Doppler-broadened cross sections are determined at every energy point in the union energy grid using NJOY-derived routines that implement Cullen's exact Doppler broadening equation [7]. These cross sections are determined for a set of temperatures, called the *fit temperature grid,* using a fit temperature interval ΔT_{fit} over the specified temperature range. The fit temperature grid is separate from the union temperature grid and while the two grids can be the same, in practice the fit temperature grid is usually much finer than the union grid. Exact Doppler-broadened cross sections are tabulated on the fit temperature grid for each energy on the union energy grid. We have used $\Delta T_{union} = 100\text{K}$ and $\Delta T_{fit} = 10\text{K}$ for the OTF cross section sets discussed in this paper.

2.4. Calculation of OTF Expansion Coefficients

Treating the expansion coefficients in Eq. (1) as the unknown variables, the expansion for a given cross section type at a given energy is evaluated for all temperatures on the fit temperature grid, yielding a system of linear equations $\boldsymbol{Ax = b}$, in which the vector $\boldsymbol{b}$ contains the cross sections at each temperature, $\boldsymbol{x}$ is the vector of the coefficients, and each row of the matrix $\boldsymbol{A}$ holds the values of the temperature corresponding to the elements in the given row raised to the powers of the expansion. This is illustrated in the following matrix representation of Eq. (1):

$$\begin{pmatrix} T_1^{-N/2} & T_1^{-(N-1)/2} & \rightleftharpoons & T_1^{(N-1)/2} & T_1^{N/2} \\ T_2^{-N/2} & T_2^{-(N-1)/2} & \cdots & T_2^{(N-1)/2} & T_2^{N/2} \\ \vdots & \vdots & \ddots & \vdots & \vdots \\ T_{N_T-1}^{-N/2} & T_{N_T-1}^{-(N-1)/2} & \cdots & T_{N_T-1}^{(N-1)/2} & T_{N_T-1}^{N/2} \\ T_{N_T}^{-N/2} & T_{N_T}^{-(N-1)/2} & \cdots & T_{N_T}^{(N-1)/2} & T_{N_T}^{N/2} \end{pmatrix} \begin{pmatrix} a_{g,1} \\ \vdots \\ c_g \\ \vdots \\ b_{g,N} \end{pmatrix} = \begin{pmatrix} \sigma(T_1, E_g) \\ \sigma(T_2, E_g) \\ \vdots \\ \sigma(T_{N_T-1}, E_g) \\ \sigma(T_{N_T}, E_g) \end{pmatrix} \quad (3)$$

Here the temperatures range from T_1 to T_{NT}, so the matrix $\boldsymbol{A}$ contains N_T rows and 2N+1 columns of temperatures raised to plus and minus half powers, the vector $\boldsymbol{x}$ contains the unknown coefficients for the cross section being fit at energy E_g, and the vector $\boldsymbol{b}$ holds the values of the cross section at each of the N_T temperatures.

Such a system typically lends itself to easy solution by a least squares minimization approach. Unfortunately, because the temperature range in OTF problems can be rather large and the expansion has both positive and negative powers of the temperature, the matrix $\boldsymbol{A}$ usually has a poor condition number and can be rank-deficient, so solving the system generally requires

singular value decomposition (SVD). In SVD, the matrix $\boldsymbol{A}$ is recast as $\boldsymbol{U\Sigma V^T}$ where $\boldsymbol{U}$ and $\boldsymbol{V}$ are orthogonal and $\boldsymbol{\Sigma}$ is a diagonal matrix containing the singular values of $\boldsymbol{A}$, which are the square of the eigenvalues. The coefficient vector $\boldsymbol{x}$ is then given by $\boldsymbol{x = V\Sigma^{-1}U^T b}$.

In the current work, the routine MINFIT from the SLATEC (EISPACK) library [8] has been adapted for FORTRAN 90 and implemented in *fit_otf* to compute the coefficients. Initially it was found that quadruple precision arithmetic was required to produce reliable fits, but it was later determined that double precision calculations would suffice if the OTF expansion was made not in terms of the temperature T but rather in terms of a scaled temperature given by $(T - T_1 - T_{off})/(T_{NT} - T_1 - T_{off})$. In this scaling, the offset temperature $T_{off} = (T_1 - T_{NT})/50$ and T_1 and T_{NT} are the upper and lower temperatures of the fit temperature grid.

Since the variation with temperature is significantly different at different energies for the same cross section and is also different at the same energy for different cross sections, the number of coefficients required for accurate modeling can vary greatly with both energy and cross section type. Therefore, the number of coefficients of the expansion is allowed to vary with both energy and cross section type.

The generation of the coefficients proceeds as follows. At a given energy in the union energy grid, exact cross section values are generated at all temperatures on the fit temperature grid for all cross sections types being fit. Starting with expansion order 1 (meaning 3 expansion coefficients), the temperature matrix $\boldsymbol{A}$ is then calculated and MINFIT is called to generate for each cross section type the least squares coefficients for the given fit-order. (Note that since $\boldsymbol{A}$ depends only on the temperatures of the fit grid and the order of the expansion coefficients, it is independent of cross section type and so the same, computationally expensive SVD procedure can be applied to all cross section types at once, rather than having to be performed independently.) Next, cross section values are calculated at each temperature in the grid using the fit coefficients and compared to the exact value for each cross section type. If any of the fitted values differ from the exact values by more than the input tolerance (the default tolerance is 0.1% relative difference, similar to the fractional tolerance in NJOY), the process is repeated using a higher order fit (but only for those cross section types not already shown to be accurately fit with a lower order expansion). Once all of the cross section types are fit to better than 0.1%, the loop over expansion order is broken and the program moves to the next union grid energy.

The *fit_otf* program utilizes multicore parallel threading to reduce computer run times. Note that this code does not replace NJOY, but supplements it, providing a convenient mechanism for extending the Doppler broadening to a wide range of temperatures.

2.5. Sensitivity Study for Union and Fit Temperature Increments

A sensitivity study on different choices of ΔT_{union} and ΔT_{fit} for U-238 was carried out by Yesilyurt and is attached as Appendix A in [6]. A brief summary is given here. It was concluded that ΔT_{union} = 50K was sufficient to maintain a fractional tolerance of .1% with a reasonable number of energy grid points over the temperature range 250K - 3200K. Also, the OTF cross sections at 1975K, midway between the union temperature points 1950K and 2000K, agreed with NJOY to within .00001%. A sensitivity study on ΔT_{fit} was also carried out and it was

concluded that ΔT_{fit} = 1K was a very conservative choice for fitting the expansion coefficients (with 17 terms) but 25K was too large, yielding a few cross sections outside the .1% fractional tolerance. It was decided to use ΔT_{fit} = 10K to obtain acceptable results with reasonable computational efficiency.

2.6. Construction of the OTF Library

The above steps have been integrated into FORTRAN 90 code *fit_otf*. The actual generation of the OTF library is dependent on a number of quantities that are user-specified:

- the list of isotopes,
- the base cross section library for each isotope,
- the temperature range over which the OTF cross sections are generated,
- the error criterion corresponding to FT,
- the temperature intervals ΔT_{union} and ΔT_{fit}, and
- the maximum order of expansion to be used for the high precision fit.

Another important consideration is the cross section types to be included in the OTF library. This decision is determined by whatever NJOY does: if a cross section type is broadened by NJOY, it is automatically included in the OTF library. The *fit_otf* code reads in the NJOY base library and identifies which of the cross section types (MT) has Doppler-broadened cross sections. The energy grid, over which these cross sections are broadened, ranges from .00001 MeV to the highest energy less than the unresolved energy range or the energy at which high threshold reactions occur, whichever is lowest. The base cross section set contains all of the temperature independent cross section information, such as the unresolved cross sections and collision physics data, for each isotope in the OTF library.

It must be noted that the OTF library and its use in MCNP address only the Doppler broadening of resolved resonances, over the same range of energies where NJOY would perform such broadening. At the present time, the OTF methodology does not cover temperature effects on either the unresolved resonances or the S(α,β) thermal scattering data. For thermal reactor systems that are the initial target for this work, the temperature effect of unresolved resonance data is very small, and can be handled by using base cross-section libraries in MCNP at the prevailing temperature of the problem. Similarly, thermal scattering datasets should be chosen for MCNP at the prevailing problem temperatures. Work is in progress to address the temperature dependence of the unresolved resonance and S(α,β) data.

2.7. Implementation of OTF Methodology in MCNP

The previous sections describe the methodology used to generate the OTF library. The number of modifications to MCNP was modest, involving only a few routines that retrieve and interpolate cross section data as a function of neutron energy. Since there is only one OTF cross section set (the set of expansion coefficients) per isotope regardless of the temperature range, the TMP cards simply designate the cell temperatures. If a given isotope is in that cell, the OTF expansion for that isotope is evaluated at that temperature. The use of TMP illustrates the substantial reduction in input complexity with OTF – a material (isotope) has the same ID in every cell in which it is found, regardless of the temperature of the cell. This is to be contrasted to the conventional

methodology where a separate material ID has to be assigned to an isotope if it is in a cell at a different temperature. This results in a proliferation of material IDs and associated cross section files for full-core simulations with TH feedback, increasing the size of the cross section files as well as increasing the complexity of the input file.

3. ASSESSMENT OF OTF METHODOLOGY

3.1. Doppler Reactivity Benchmark Suite

The Doppler reactivity benchmark suite [9] was chosen for the first comparison of the OTF methodology versus the conventional approach using ACE cross sections generated at the specific temperatures. This problem compares keff for HZP (hot, zero power) and HFP (hot, full power) conditions for a typical PWR fuel pin cell with three regions – fuel, clad, and moderator. For the HZP cases, all regions are at 600K. For the HFP cases, the fuel region is at 900K while the clad and moderator regions remain at 600K. There are three different fuel regions: UO2, MOX with reactor-grade plutonium, and MOX with weapons-grade plutonium. There is a range of uranium enrichments for the UO2 cases and a range of PuO2 weight percent for the MOX cases. Simulations were performed using 10,000 cycles (9500 active) of 10,000 histories for each benchmark case. Tables I and II presents comparisons of MCNP results using OTF cross sections and conventional ACE cross sections for UO2 and reactor-grade MOX cases, respectively. (The weapons-grade MOX cases were not analyzed.)

Table I. Comparison of OTF versus Standard Method for the UO2 Cases

Enrichment	Method	keff (one σ)		Doppler Defect (one σ) (pcm/K)	
		HZP	HFP	MCNP	Avg [9]
.711%	OTF	0.66564 (04)	0.65973 (04)	-4.486 (43)	-4.27
	Std	0.66565 (04)	0.65975 (04)	-4.478 (43)	-4.27
1.6%	OTF	0.96084 (06)	0.95273 (06)	-2.953 (31)	-3.00
	Std	0.96091 (06)	0.95261 (06)	-3.022 (31)	-3.00
2.4%	OTF	1.09914 (06)	1.08991 (06)	-2.568 (24)	-2.52
	Std	1.09904 (06)	1.08996 (06)	-2.527 (24)	-2.52
3.1%	OTF	1.17713 (06)	1.16751 (06)	-2.333 (21)	-2.30
	Std	1.17719 (06)	1.16749 (06)	-2.353 (21)	-2.30
3.9%	OTF	1.23974 (06)	1.22975 (06)	-2.184 (19)	-2.20
	Std	1.23973 (07)	1.22966 (07)	-2.202 (22)	-2.20
4.5%	OTF	1.27516 (06)	1.26510 (06)	-2.079 (18)	-2.18
	Std	1.27514 (07)	1.26503 (07)	-2.089 (20)	-2.18
5.0%	OTF	1.29900 (07)	1.28933 (07)	-1.925 (20)	-2.06
	Std	1.29897 (07)	1.28924 (06)	-1.937 (18)	-2.06

The results in Tables I and II clearly indicate that the OTF methodology is working correctly, providing results that agree with conventional MCNP calculations within statistics.

For these simple pin cell runs, MCNP with OTF cross sections had a performance penalty of 15-20% compared with conventional ACE cross sections. For this modest number of isotopes and temperatures, the memory required to store cross sections was slightly larger with OTF than with ACE cross sections. However, the same OTF library can be used for the radial temperature dependent case that follows, which is not the case with the temperature-specific ACE cross sections.

Table II. Comparison of OTF versus Standard Method for the PuO2 Cases

Enrichment	Method	keff (one σ)		Doppler Defect (one σ) (pcm/K)	
		HZP	HFP	MCNP	Avg [9]
0.0%	OTF	0.66564 (04)	0.65973 (04)	-4.486 (43)	-4.27
	Std	0.66565 (04)	0.65975 (04)	-4.478 (43)	-4.27
1.0%	OTF	0.94493 (06)	0.93520 (06)	-3.670 (32)	-3.72
	Std	0.94483 (06)	0.93515 (06)	-3.652 (32)	-3.72
2.0%	OTF	1.02069 (07)	1.00973 (07)	-3.545 (32)	-3.60
	Std	1.02071 (07)	1.00969 (07)	-3.564 (32)	-3.60
4.0%	OTF	1.07588 (07)	1.06410 (07)	-3.430 (29)	-3.50
	Std	1.07577 (07)	1.06414 (07)	-3.386 (29)	-3.50
6.0%	OTF	1.10457 (07)	1.09271 (07)	-3.275 (27)	-3.30
	Std	1.10451 (07)	1.09280 (07)	-3.234 (27)	-3.30
8.0%	OTF	1.12790 (07)	1.11606 (07)	-3.135 (26)	-3.20
	Std	1.12793 (07)	1.11607 (07)	-3.140 (26)	-3.20

3.3. Doppler reactivity benchmark suite with radial temperature dependence

The first set of test problems verified the OTF methodology. The second set of test problems is identical to the first set except the fuel region is divided into radial rings with different temperatures. The purpose of this set of test problems is to illustrate the relative ease of setting up temperature-dependent cases with OTF cross sections. These test problems also show the impact of modeling the radial temperature distribution in detail on the Doppler coefficient. A radial temperature distribution $T(r) = 1200 - 600\left(r / R\right)^2$ was imposed in the fuel region, consistent with a fuel pin of radius R with 900K average fuel temperature and 600K fuel surface temperature. With this temperature distribution, the average fuel temperatures in the 10 rings are given in Table III, where ring #1 is on the centerline of the fuel pin. For convenience, it was

assumed that the number densities in the fuel did not vary with temperature and were equal to the 900K densities from the first test problem.

Table III. Average Fuel Ring Temperatures

Ring #	1	2	3	4	5	6	7	8	9	10
Temp (K)	1197	1185	1160	1125	1077	1016	944	861	764	656

This simulation was quite simple to perform with the OTF cross sections. The only changes that had to be made to the MCNP input files for the uniform temperature cases were to specify the temperatures for the ten fuel regions. With the conventional ACE cross section files, the user has to assign to each radial region an ACE cross section set for each isotope at the corresponding temperature. In that case, the number of MCNP input cards would have increased by a factor of 13 over the number required with OTF cross sections.

The radially dependent pin cell cases were not run with conventional ACE files because the OTF methodology was already verified for the pin cell cases in the previous section and it would have been a considerable burden to prepare the cross section files and the MCNP input files. However, it is interesting to see the impact of the radial variation in temperature on the Doppler coefficient. Figure 3 plots the Doppler coefficients for the UO2 pin cell problems as a function of enrichment for the uniform temperature cases versus the radially-dependent temperature cases, along with the benchmark results [9]. Similar results were obtained for the PuO2 cases and can be found in [6]. For all cases, the effect of the radially-dependent temperatures is a small reduction in the magnitude of the Doppler coefficient. This phenomenon is well-known but has been cumbersome to analyze with Monte Carlo due to the difficulty of dealing with temperature-dependent cross section files. The OTF methodology allows this type of analysis to be performed easily.

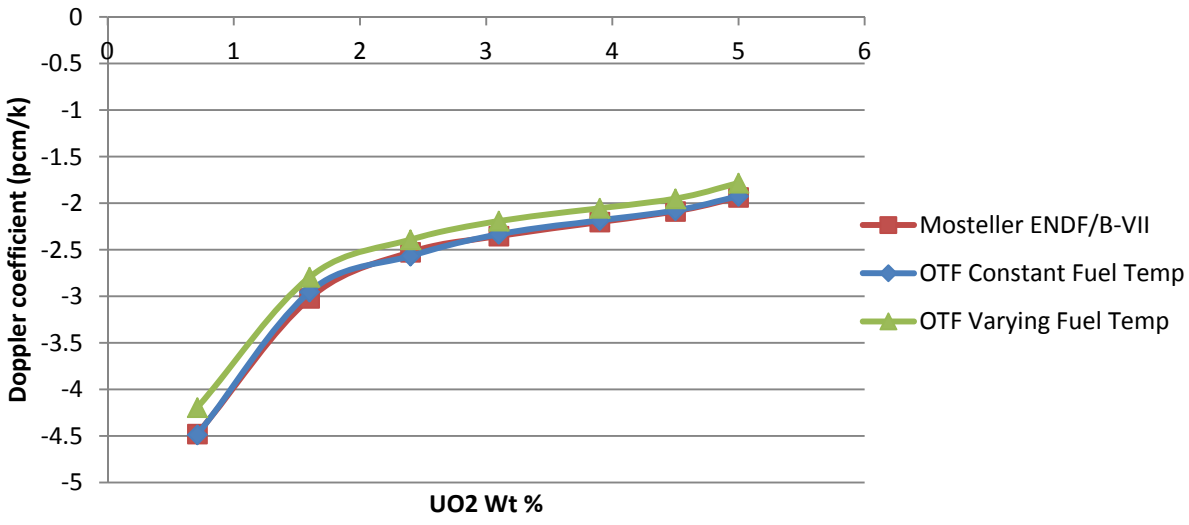

Figure 3. Doppler Reactivity Defect for UO2 Benchmark Cases

3.4. Full core VHTR with imposed temperature distribution

This test problem is based on the full-core Very High Temperature Reactor (VHTR) with an imposed temperature distribution that in turn was taken from a coupled neutronic/thermal-hydraulic (NTH) simulation [10] of the VHTR using MCNP for the neutronic analysis and RELAP5-3D/ATHENA [11] for the thermal-hydraulic (TH) analysis. The goal of this earlier analysis was to determine the beginning-of-cycle (BOC) power and temperature distributions for the VHTR core at the rated power of 600 MWt. Figure 4 depicts the VHTR configuration analyzed in this earlier study. Figure 5 shows the temperature-dependent regions that are used.

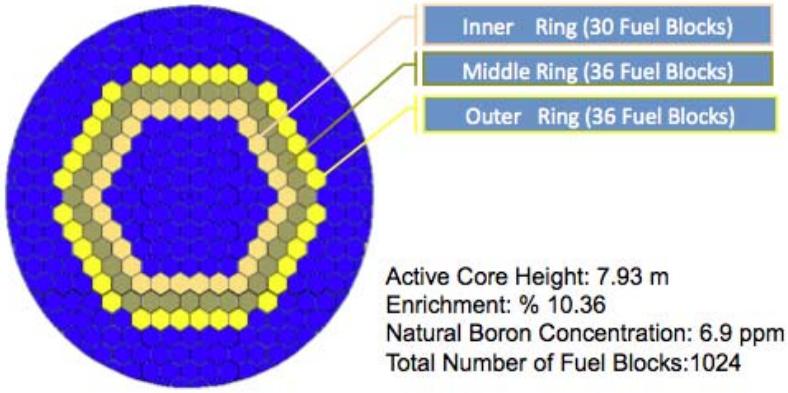

Figure 4. Full-Core VHTR Configuration

Iref	Iring	Mring	Oring	Oref
1	1	1	1	1
2	2	2	2	2
3	3	3	3	3
4	4	4	4	4
5	5	5	5	5
6	6	6	6	6
7	7	7	7	7
8	8	8	8	8
9	9	9	9	9
10	10	10	10	10
11	11	11	11	11
12	12	12	12	12

Legend	
1	Core Inlet Plenum
12	Core Outlet Plenum
Iref	Inner Reflector
Iring	Inner Ring of Core
Mring	Middle Ring of Core
Oring	Outer Ring of Core
Oref	Outer Reflector

Figure 5. Map of the VHTR Core.

To avoid generating a large number of ACE files, the VHTR test problem was simplified by averaging the converged temperature distributions from the earlier analysis [10] over larger regions. The resultant temperature distribution in degrees K is given in Table IV, where the region numbers correspond to the VHTR map in Figure 5. This simplified temperature distribution still required generation of 52 ACE files, taking into account similar temperatures in different regions for the same isotopes. This is to be compared with 7 cross section files needed

with OTF. The results of two MCNP simulations are shown in Table V. The observed difference in keff for these two cases is negligible.

Table IV. Imposed Temperature Distribution for VHTR Test Problem

Axial #	Iref	Iring	Mring	Oring	Oref
1	900	900	900	900	900
2	900	900	900	900	900
3	900	1100	1100	1100	900
4	900	1100	1100	1100	900
5	900	1100	1100	1100	900
6	1100	1350	1250	1300	1100
7	1100	1350	1250	1300	1100
8	1100	1350	1250	1300	1100
9	1100	1450	1300	1350	1100
10	1100	1450	1300	1350	1100
11	1100	1400	1250	1250	1100
12	1100	1400	1250	1250	1100

Table V. Comparison of Results using MCNP with OTF vs. Conventional Cross Sections

Case	#Active cycles	Particles per cycle	keff	σ	Δkeff
Conventional	400	100,000	1.15616	.00014	--
OTF	400	100,000	1.15614	.00014	.00002

3.5. Full core VHTR with thermal-hydraulic coupling

This VHTR test problem is a coupled nuclear/thermal-hydraulic (NTH) calculation with MCNP and RELAP5-3D/ATHENA (RELAP5). In this case, the generation of ACE files for the coupled problem is no longer practical because the temperatures in the 60 regions are not known *a priori* and it would take 300 NJOY runs *during each NTH iteration* to generate the ACE libraries at all the temperatures that may be encountered in the 60 regions. For that reason, we decided to use the pseudo materials method [12], as was done in [10], to account for temperature feedback within MCNP.

To provide the cross sections needed for the pseudo materials method, ENDF/B-VII library files for MCNP were prepared using NJOY99 (update 364) for isotopes B-10, B-11, and C-12 at every 100K from 700K to 2400K. For isotopes U-235, U-238, O-16, and Si-28, temperature-dependent library files were generated at every 100K from 900K to 2400K, giving a total of 125 MCNP library files and 1.6 GB of data. For the lighter elements, generation of the data files took just several minutes, but, because of the need to generate probability tables for determining cross

sections in the unresolved resonance region for the heavier materials, several hours of computation time on quad-core processors were required to prepare data for each heavy isotope.

Data files were also prepared for OTF cases in the temperature range 600K to 3000K based on standard MCNP libraries. Again, data preparation computation times were minimal for low Z materials, increasing to approximately 40 minutes for U-235 and two hours for U-238, because of the large number of energy grid points. The total size of the OTF libraries was 359 MB, less than ¼ of that needed for the pseudo-materials method, which itself requires considerably less memory than needed to generate ACE cross sections files every 10K or 20K. Temperatures for moderator S(α,β) data were fixed at 1200K in the fuel, and 1000K in the reflectors. Because of the temperature variation in each region, each cell in the pseudo material implementation was a unique MCNP input material, requiring a total of 668 cards. In contrast, the MCNP input file using OTF only required 16 cards to specify the materials.

MCNP runs used 200,000 histories per cycle and 600 cycles, discarding the first 200, and required roughly 5 hours on 16 cores at the University of Michigan (UM) cluster. Details of the coupling methodology and convergence testing are given in [10]. Figure 6 shows the progression of keff with iteration. For both the pseudo material case and the OTF Doppler runs, convergence of keff was achieved after roughly 5 iterations. Average values of keff for iterations 6 through 15 were 1.14697 for the OTF computation and 1.14694 for the pseudo material case, a difference of 3 pcm. It is clear that the OTF Doppler and pseudo material simulations predict very similar results for keff as a function of the NTH iteration.

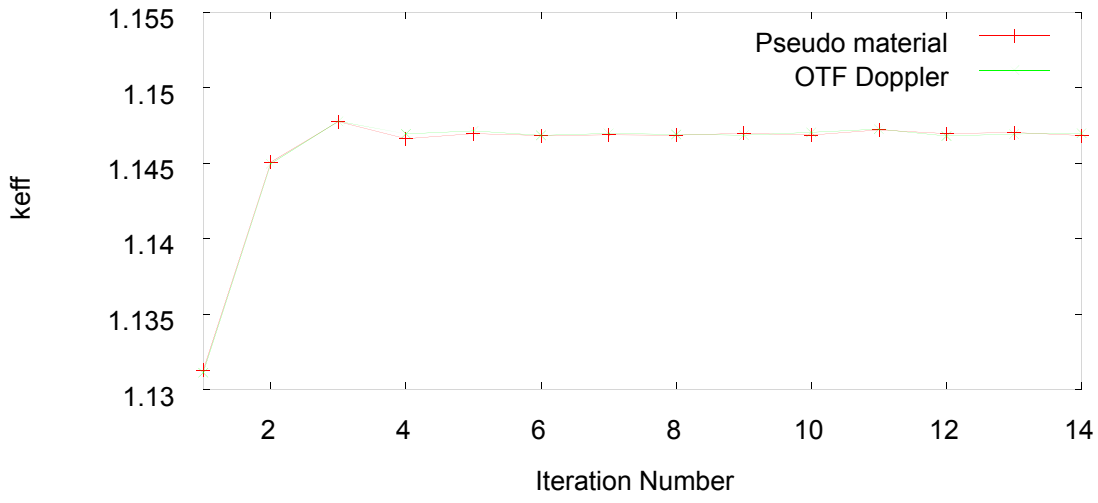

Figure 6. VHTR keff versus Cycle for OTF and Pseudo Materials.

These results clearly show that the OTF cross section capability in MCNP is generating consistent temperatures throughout the full-core geometry. The convergence trends are the same for both methods for the NTH iteration and the converged keff is essentially the same. From a performance standpoint, the computing time was a little higher (~ 10%) for OTF versus pseudo materials. However, the input complexity is substantially reduced with OTF and the size of the cross section files is also reduced. Specifically, the size of the cross section files for the coupled

VHTR test problem was 359 MB for OTF and 1.6 GB for pseudo materials. If pseudo-materials were not used for the VHTR problem, the size of the cross section files would have been 8 GB, assuming a cross section file for every 10K. For the coupled VHTR test problem, using OTF to model the temperatures exactly only requires the user to update the TMP values of all 60 cell cards in the MCNP input deck to reflect the new temperatures computed in RELAP. No additional input modifications are needed when using the OTF methodology.

4. Summary and Conclusions

The OTF methodology has been successfully implemented into the MCNP Monte Carlo code. A special version of MCNP5 was developed and used for all of the OTF-based runs described in this work. The OTF methodology has been implemented in a beta-release version of MCNP, MCNP6-beta-3, that will be released by RSICC in early 2013. The production release version of MCNP6 is targeted for spring/summer 2013 and will include OTF Doppler broadening.

The OTF cross sections agree to within a specified fractional tolerance (FT) with the NJOY-based cross sections for all neutron energies and all temperatures specified by the user, e.g., 250K - 3200K. The *fit_otf* code generates the OTF library and can be used to generate additional OTF libraries as needed. Currently, the methodology addresses only the resolved resonance Doppler broadening, which is most important for thermal reactors. Additional work is in progress to include unresolved resonances (important for fast systems) and S(α,β) data.

Specific OTF libraries have been developed to analyze the test problems described in this report. A separate OTF library covering the temperature range 250K – 3200K is being generated using *fit_otf* that contains the following isotopes: H-1, H-2, B-10, B-11, C-12, O-16, Si-28, Fe-54, Fe-56, Fe-57, Fe-58, Zr-90, Zr-91, Zr-92, Zr-94, Zr-96, Xe-135, Sm-149, Gd-155, Gd-157, Th-232, U-233, U-234, U-235, U-238, Pu-239, Pu-240, Pu-241, and Pu-242.

The accuracy of the OTF methodology has been assessed with several test problems by comparing MCNP runs with both conventional cross section files and OTF cross section files. The test problems include the Doppler defect reactivity benchmark suite and two full-core VHTR configurations, including one with multiphysics coupling using RELAP5-3D/ATHENA for the thermal-hydraulic analysis. The comparison has been excellent, verifying that the OTF libraries can be used in place of the conventional ACE libraries generated at problem temperatures.

The use of OTF cross sections greatly reduces the complexity of the input for MCNP, especially for temperature feedback calculations with many regions at different temperatures. This is due to the fact there is only one cross section file for each isotope, regardless of the number of temperatures the isotope may experience. This results in an order of magnitude decrease in the number of input lines for full-core configurations, thus simplifying input preparation and reducing the potential for input errors.

The use of OTF cross sections can lead to a substantial reduction in the size of the cross section files needed to carry out MCNP simulations with multiphysics feedback. This is due to needing only one cross section file per isotope, rather than per isotope-temperature. A ballpark estimate of the savings can be obtained by noting that a typical OTF cross section file for a given isotope

may be equivalent to storing cross section files at 10-15 temperatures, depending on the isotope. For multiphysics simulations where cross sections may be needed every 10K, this is a huge savings in memory.

The additional computational effort to use OTF cross sections is modest (10-15%) for large problems such as the full-core VHTR problems and somewhat higher for smaller problems such as the pin cell problems.

ACKNOWLEDGMENTS

The work reported in this paper was supported by DOE NEUP contract DE-AC07-05ID14517.

REFERENCES

1. X-5 Monte Carlo Team, "MCNP - A General N-Particle Transport Code, Version 5, Volume I: Overview and Theory," LA-UR-03-1987, Los Alamos National Laboratory (2003).
2. R. E. MacFarlane and D. W. Muir, "NJOY99.0 - Code System for Producing Pointwise and Multigroup Neutron and Photon Cross Sections from ENDF/B Data," PSR-480/NJOY99.00, Los Alamos National Laboratory, Los Alamos (2000).
3. G. Yesilyurt, "Advanced Monte Carlo Methods for Analysis of Very High Temperature Reactors: On-the-Fly Doppler Broadening and Deterministic/Monte Carlo Methods," PhD thesis, Department of Nuclear Engineering and Radiological Sciences, University of Michigan, Ann Arbor, MI (2009).
4. G. Yesilyurt, W. R. Martin, and F. B. Brown, "On-the-Fly Doppler Broadening for Monte Carlo Codes," *Nucl. Sci. Eng.* **171**, 239-257 (2012).
5. F. B. Brown, W. R. Martin, G. Yesilyurt, and S. Wilderman, "Progress with On-The-Fly Neutron Doppler Broadening in MCNP," *Trans. Am. Nucl. Soc.* **106**, 508-510, Chicago, IL (June 2012).
6. W. R. Martin, G. Yesilyurt, F. B. Brown, and S. Wilderman, "Implementation of On-the -Fly Doppler Broadening in MCNP5 for Multiphysics Simulation of Nuclear Reactors," www.osti.gov/servlets/purl/1058919/ , Final Report for NEUP Project 10-897, Contract DE-AC07-05ID14517, U. S. Department of Energy (2012).
7. D. E. Cullen and C. R. Weisbin, "Exact Doppler Broadening of Tabulated Cross Sections", *Nucl. Sci. Eng.*, **60**, 199-229 (1976).
8. B. T. Smith, J. M. Boyle, J. J. Dongarra, B. S. Garbow, Y. Ikebe, V. C. Klema and C. B. Moler, *Matrix Eigen-system Routines - EISPACK Guide*, Springer-Verlag,1976.
9. R. D. Mosteller, "The Doppler-Defect Benchmark: Overview and Summary of Results," *Proc. Joint Int. Topical Mtg on Mathematics and Computation and Supercomputing in Nuclear Applications, M&C + SNA 2007*, American Nuclear Society, Monterey, CA (2007).
10. G. Yesilyurt, K. Banerjee, E. Villèle, J.C. Lee, and W.R. Martin, "Coupled Nuclear-Thermal-Hydraulic Calculations for VHTRs," *Trans. Am. Nucl. Soc.* **102**, 519-521, San Diego, CA (June 2010).
11. RELAP5-3D Code Development Team, *ATHENA Code Manual*, *INEEL-EXT-98-00834, Rev. 2.2*, Idaho National Engineering and Environmental Laboratory (2003).
12. J. L. Conlin, W. Ji, J. C. Lee, and W. R. Martin, "Pseudo Material Construct for Coupled Neutronic-Thermal-Hydraulic Analysis of VHTGR," *Trans. Am. Nucl. Soc*. **92**, 225 (2005).